Ionic distribution around simple B-DNA models. III. The effect of ionic charge

José L. F. Abascal[a] and Juan Carlos Gil Montoro
Departamento de Química-Física, Facultad de Ciencias Químicas, Universidad Complutense de Madrid, E-28040 Madrid, Spain

(Received 8 August 2000; accepted 27 November 2000)

The effect of the ionic charge on the ionic distribution around a simple B-DNA model at the continuum solvent level is investigated using Monte Carlo simulation. In the model, the DNA shape is approximated by a set of simple geometric elements with charges at the canonical phosphate positions. Three series of simulations for an infinitely diluted polyion with added salt have been carried out. In each of them the ionic strength is kept constant. At low ionic strength, the behavior of monovalent, divalent, and trivalent cations is studied. It is shown that the number of counterions within the grooves depend only weakly on its valence so the fraction of DNA charge canceled out at small distances increases with the charge of the cation. This results in a deeper penetration of the coions, which, for systems with highly charged counterions as a 3:1 salt, may even surpass the bulk concentration in the vicinity of the polyelectrolyte. Nevertheless, no overscreening of the DNA charge has been observed in this system. On the contrary, the charge reversal phenomenon appeared in the simulations at high ionic strength irrespective of the ionic valences. It seems that this feature occurs when the bulk concentration of the mobile ions is of the same order as the local concentration in the vicinity of DNA with no added salt. Finally, the competition between monovalent and divalent cations is studied at concentrations close to those of biological media. It is shown that the divalent cations push the monovalent ions out of the DNA surroundings even if their concentration is much lower. [DOI: 10.1063/1.1342035]

I. INTRODUCTION

This is the third of a series of papers devoted to the study by computer simulation of the ionic atmosphere around simple B-DNA models within a continuum solvent approximation. In the first one[1] (paper I) we examined the cylindrically averaged properties obtained for several models. In a further study[2] (paper II) we dealt with the departures of the ionic atmosphere from the cylindrical symmetry. In this paper we investigate the ionic distribution around DNA in the presence of multivalent ions. The analysis in Papers I and II showed that the interplay between the electrostatic forces dues to the helical arrangement of charges with the repulsive forces that determine the DNA shape explains the main features of the binding of monovalent ions to DNA and gave a strong support for the validation of the so-called grooved primitive (GP) model. The ability of the GP model to mimic features previously found only in all-atom models as the double peak in the concentration profile as well as to explain experimental results such the ζ potential[3] or the thermodynamics of the B to Z–DNA transition and its dependence on the ionic concentration[4,5] is a confirmation of the suitability of the model in problems that are currently beyond the scope of all-atom DNA simulations. In the last years, there is an increasing number of computer simulations of all-atom DNA solutions with added salt; see, e.g., Refs. 6 and 7. These studies use a limited number of ions, typically some tens, and are focused on the ion binding to specific places close to the polyion, in particular, the occupancy of electronegative pockets by counterions. But the detailed spatial distribution of ions at a certain distance to DNA is still out of the reach of all-atom model simulations, especially when a small fraction of divalent counterions compete with the monovalent ones. In contrast, the simulations using the GP model may include a vast number of counter- and coions.

The model also has obvious limitations (neglect of the molecular nature of the solvent and no consideration of sequence specific effects), though this is not necessarily a drawback in some cases. In this series, we have deliberately adopted a simple model approach since this allows us to learn the physics that a given refinement adds with respect to a previous level, thus unambiguously assigning each effect to its cause. Another advantage of the use of simple models is that the significance of the results goes beyond the specific case of DNA and concern general properties of polyelectrolyte solutions. In this respect, a challenging problem is that of the *attraction* between negatively charged macromolecules. There is now considerable experimental[8,9] and Monte Carlo[10,11] evidence of this phenomenon in DNA and other charged biopolymers.[12] Recent Brownian dynamics simulations of a system of two like-charged rods[13] also show that the attraction is mediated by counterions and molecular dynamics simulations[14] indicate that divalent counterions induce the formation of bundles in stiff polyelectrolytes and DNA condensation.[15] Notice that the limitation in the number of coions in all-atom simulations disables the investigation of this type of phenomena that may be necessarily ap-

[a]Electronic mail: jl@juguete.quim.ucm.es

proached with simpler models. In this paper we try to cover both aspects of the properties of DNA solutions. On the one hand, we are interested in the ''binding'' of multivalent ions to DNA in conditions more or less similar to those of physiological environments. Besides, the study is complemented with the study of several features of the ionic profiles that can be related to the counterion mediated attraction of macroions.

Although 1:1 salts have been extensively studied, only a few results have been obtained for highly charged ions near a rigid polyion. Earlier investigations were carried out with the Poisson–Boltzmann (PB) equation[16] and the Manning counterion condensation (CC) theory.[17] Monte Carlo simulations[18,19] have shown considerable discrepancies with PB calculations when divalent counterions are involved. In paper II we also showed that the finite difference Poisson–Boltzmann equation is also unable to explain important features of the spatial distribution of monovalent ions around the GP model of DNA, even at moderate salt concentrations. This is because in the PB equation, the counterion and coion concentration depend on the electrostatic field created in that point by the polyelectrolyte and its average ionic envelope, thus neglecting the correlations between mobile ions. In fact, a simple scaling through the Boltzmann factor is the only difference between the PB predictions for different ionic charges. The failure of the PB equation is magnified when the solution contains highly charged counterions. This has been shown by the results of more elaborated theories and their comparison against computer simulation results. Among the successful theories, we should cite the hypernetted integral equation[20] and, especially, the modified Poisson–Boltzmann equation (MPB) based on the Kirkwood hierarchy.[21–23] The implementation of these theories for arbitrary molecular shapes is complicated and has been generally restricted to the planar, spherical, and cylindrical geometries. The MPB theory has also been applied to macromolecules with nontrivial shapes such as proteins (within a formulation using the Bogolyubov–Born–Green–Yvon hierarchy[24]) and B-DNA.[25] Unfortunately, the method is computationally very expensive. In fact, the calculations reported in the latter reference required several hours on 16 processors of a CRAY T3E computer. This is to be compared with the time required by any of the simulations reported in the present paper for a model reproducing the approximate DNA shape which was about 5 h in a Pentium II at 350 Mhz. At present, it should be questionable the use of an approximate theory in a situation where a Monte Carlo simulation can yield essentially ''exact'' results with a comparable (or less) computational cost. But the advantage of the macroscopic approach made in the MPB theory is that it allows us to incorporate the different dielectric constants for both the interior of the polyion and the surrounding solvent. Thus, theory and simulation are complementary techniques. Interestingly, in the particular case of DNA, Gavryushov and Zielenkiewicz[25] have shown that the influence of the dielectric discontinuity on the electrostatic potential at the charged DNA groups is weak even in the presence of a concentrated—ionic strength 0.5 M—2:1 electrolyte. This gives strong support to continuum solvent Monte Carlo simulations, where the effects of the dielectric discontinuity cannot be easily taken into account.

The paper is organized as follows. In Sec. II we summarize the methodology employed in this work. The results are presented in Sec. III; the calculations for multivalent ions at low and high ionic strength are given in Secs. III A and III B, respectively, and the results for the competition of ions with different charges appear in Sec. III C. The implications of this work are summarized in Sec. IV.

II. METHODOLOGY

In the grooved primitive model, the DNA shape is approximated by means of simple geometric elements. The procedure is discussed in detail in paper I. As most of the DNA charge lies at the phosphate groups,[26] unit negative charges are placed at the phosphorus positions.[27,1] A cylinder mimics the central core of DNA, totally inaccessible to the mobile ions, while each nucleotide is completed by two identical spheres, one of them centered at the charged groups, and the other one lying between the phosphates and the cylinder at a radial coordinate $\rho = 5.90$ Å. Irrespective of whether the charges are fixed (the polyelectrolyte sites) or mobile (the solution particles), the repulsive interaction between them is a soft potential that depends on the distance as r^{-n} with $n=9$. The ionic diameters are chosen so that they are approximately equivalent to a hard sphere of 4.2 Å, which roughly corresponds to a sodium ion with the account of its hydration shell. Additionally, the intermediate spheres of the GP model interact with the mobile ions through the same potential. The repulsive interactions between the central cylinder and the mobile ions also depends on an inverse ninth power. The peculiarity is that the distances are not relative to the helix axis but they are shifted by 2.91 Å, which gives an effective grooves depth of about 3.9 Å.

We use the Coulombic potential—without further modification beyond the mere consideration of the dielectric constant of water at 25 °C—for the electrostatic interactions between mobile ions. All calculations correspond to a polyion at infinite dilution in a salt solution of specified bulk concentrations. Our calculations assume an infinitely long and rigid DNA and, thus, the replication along the cell boundaries must be treated accordingly. The electrostatic interaction between a mobile ion and the DNA charges is then the sum of the potential between the ion and several infinitely long arrays of discrete charges along lines parallel to the DNA axis.[28] The mobile ions outside the simulation box along the axial direction are taken into account using the mean concentration profiles.

Two different methods have been employed for the periodic boundary conditions along the radial direction. At low ionic strengths, the traditional cell model[29] is used. More concentrated salt solutions can be affected by the presence of the hard boundary,[30] especially when the solution contains a mixture of ions with different charges.[31] For these systems, the modulated bulk as a fuzzy boundary (MBFB) method[30,31] has been used instead. In this method, the cylinder corresponding to the cell model (the inhomogeneous region) is immersed in a periodic box (a hexagonal prism in our case) filled with bulk solution and the hard wall removed, so that

TABLE I. The simulations.

Salt type[a]	Bulk ionic strength (M)	Number of counterions[b]	Number of coions	Radial boundary	Radial dimension (Å)[c]
1:1	0.0219	80+110	110	Cell	146.7
2:1	0.0233	50+30	60	Cell	113.4
3:1	0.0204	40+30	90	Cell	153.2
1:1	4.45	20+200	200	MBFB	22.5
2:1	3.72	20+190	380	MBFB	29.5
2:2	3.80	20+205	205	MBFB	32.5
1:1	0.1	60+120	120	Cell	81.3
2:1:1	0.117	60+90+15	120	Cell	75.5
2:1:1	0.124	60+60+30	120	Cell	75.5

[a]The last number indicates the charge of the anions.
[b]Counterions that cancel DNA charge + added salt cations (ordered by an increasing charge for the salt mixtures case).
[c]Cell radius in the cell model simulation or internal region radius in the MBFB simulations.

mobile ions are able to cross the boundary. The ions interact with the surrounding bulk through a discrete particle–particle modulated (short-ranged) Coulomb potential[32] while the missing tail is recovered as a mean field contribution computed in a self-consistent way.

Three sets of Monte Carlo simulations have been carried out. In each of the series the ionic strength is kept constant. The first one is intended to investigate the effect of the counterion charge at low salt. In another series, both the charges of the counterions and coions are modified in systems at high ionic strength. Finally, the third set includes two mixtures of monovalent and divalent counterions in order to study the competition between ions as a function of its charge. The simulated states are given in Table I. As a result of the inhomogeneity of the system at equilibrium, it is not possible to establish in advance the exact bulk ionic strength, i.e., that observed in the simulation far away from the polyelectrolyte. Nevertheless, the differences within a given set are not important, at least not as much as to disable their comparison. For simplicity, in the remainder of this paper, we will refer to each of the series by a rounded value close to the bulk ionic strength of the simulations.

In the salt concentrated systems, classical Metropolis sampling has been used. Convergence problems of the Markov chain can occur in diluted systems. This is again due to the strong inhomogeneity of the counterion distribution, which changes from about one molar concentration near DNA to the corresponding bulk value, which may be several orders of magnitude smaller at low added salt concentrations. To deal with this problem, a density scaled sampling scheme has been used.[33] In this method, the ion trial displacement parameter varies with the distance to the polyelectrolyte; it is small near it, and large far away.

III. RESULTS

A. Systems at low ionic strength

The ionic concentration profiles around DNA with 1:1, 2:1 and 3:1 added salt at low ionic strength (about 0.02 M) are shown in Fig. 1. These are angular averaged concentrations that depend only on the radial distance to the polyion axis. The counterion profiles exhibit a maximum, more or less split in a double peak, around the radial coordinate of the charged phosphates. The first maximum at about 8 Å corresponds to counterions located inside the DNA grooves, while the second at 12 Å is due to the cations that associate mostly in front of the phosphates.[1] The second peak has a lower height than the first one, especially for the systems with higher ionic charges, where it becomes a simple hump of the main maximum. The positions of the maxima are coincident with those exhibited by Na^+ in recent all-atom B–DNA simulations.[7] In contrast with this observation, it has been shown[18] that, when the charges were helically arranged but embedded on the surface of a cylinder, the radial profile was not much different from that found when the charges were situated in the axis. Besides, we have also shown[1] that a model with the same shape as the GP and the charges placed on the axis gives essentially the same results as the cylindrical model. In summary, neither the helical disposition of the polyion charges nor the DNA shape can alone bring the peculiar features of the spatial distribution of ions around DNA that are induced by the coupling of both structural elements.

The height of the main hump of the counterion concen-

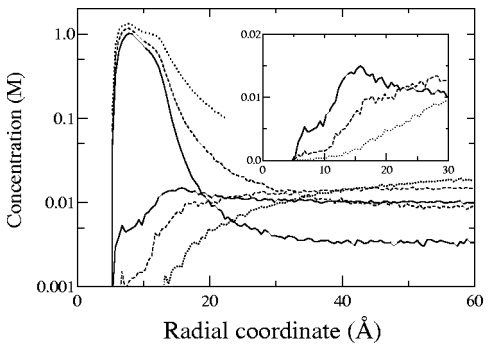

FIG. 1. Concentration profiles for systems containing 3:1 (full lines), 2:1 (dashed), and 1:1 (dotted) added salts at 0.022 M ionic strength. Upper curves are for counterions and lower for coions. Notice that the scale is logarithmic. The inset shows an enlargement of the region in which the coions concentration of the 3:1 system exhibits a maximum.

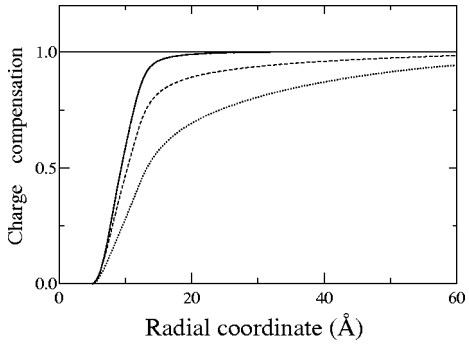

FIG. 2. Charge compensation functions for systems containing 3:1 (full lines), 2:1 (dashed), and 1:1 (dotted) added salts at 0.022 M ionic strength.

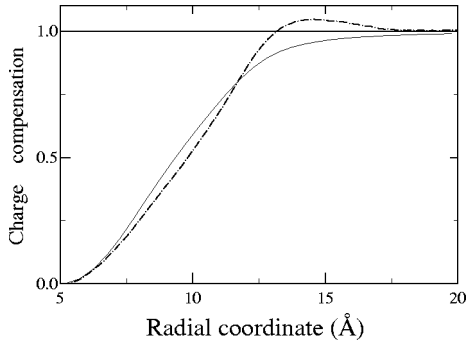

FIG. 3. Charge compensation functions for systems containing 3:1 (full line) and 1:1 (dashed–dotted) added salts at 0.022 and 4 M ionic strength, respectively.

tration profiles is of the same order for the three salts, ≈ 1 M, despite the differences in their ionic charges. It seems that, when the ionic strength is kept constant, the increase of the attractive electrostatic potential for mobile ions with higher valences is somewhat counterbalanced by the larger cost needed to keep the stronger concentration gradient due to the smaller bulk concentration of the cations. At about 12 Å from the DNA axis, the curves begin to decline exponentially to eventually reach the corresponding bulk values. The degree of penetration of the coions increases with the ionic charge of the accompanying counterion. In fact, the anion concentration profile of the system with 3:1 salt is half the bulk one *within the grooves* and reaches the bulk value at only 12 Å. Moreover, as the incorporation of coions continues outside the DNA core, the concentration profile eventually reaches a maximum at about 15 Å (see the inset in Fig. 1). Notice that, although the counterion concentration at the maximum does not depend on its charge, the fraction of DNA charge canceled out *does increase* with the charge of the mobile cations (see Fig. 2). Thus, the coions of the 3:1 salt perceive a noticeably screened polyion. Besides, the condensed trivalent cations exert a strongly electrostatic attraction on them. In this way, the formation of phosphate–counterion–coion saline bridges would explain the existence of the maximum in the coions concentration profile.

The charge compensation functions, which give an account of the fraction of DNA charge neutralized by the counterions, are represented in Fig. 2. The initial slope of the charge compensation functions increases with the ionic charge. The fraction of DNA charge canceled within the grooves—i.e., at the radial position of the phosphates—is roughly 45% for the trivalent system, 35% for the divalent cations, and only 20% for the monovalent ions. Notice also that the behavior of the divalent cations is closer to that of the trivalent than to the monovalent counterions (this was somewhat masked in Fig. 1 owing to the logarithmic scale). On the other hand, the larger the initial charge compensation, the smaller the accumulation of counterions outside DNA. This explains that the main peak splitting blurs when the counterion charge increases.

Despite the great charge density around the polyion created by the trivalent cations, the charge compensation function does not show overneutralization as it was observed for monovalent salts at high salt concentration.[1] In Fig. 3 we compare the results for the 3:1 system at 0.02 M ionic strength with those for a monovalent salt at high—4 M—concentration. The trivalent counterions cancel more quickly, i.e., at smaller distances, a substantial fraction of the DNA charge, despite the fact that their bulk concentration is three orders of magnitude smaller than that of the monovalent cations. Outside DNA the situation changes and the slope of the function decreases for the former counterions while it increases for the latter. The final result is that the curve for the solution at high ionic strength goes beyond unity—indicating the overscreening of the DNA charge—whereas the low concentrated solution does not show charge reversal.

Previous plots represented in all cases cylindrical averages. But, the simplicity of the GP model allows the simulation of a system containing several hundreds of ions, which allows a precise calculation of the corresponding spatial distribution functions. Since the system has helical symmetry, only two independent coordinates are required. In paper II we suggested these coordinates to be the radial distance to the axis and the axial distance to a reference helical line that passes through the phosphate positions. The axial coordinate can be taken either as the angular separation or, equivalently, as the distance along the Cartesian z coordinate from the reference helical line. A detailed description of the helical projection is given in Ref. 2 and it is sketched in Fig. 4 together with the results for the distribution of counterions in the 3:1 added salt system. Although the general trends are similar to those reported for monovalent salt solutions at 1 M ionic strength,[2] it is to be pointed out that the ratio between the counterion concentration in the minor groove with respect to that in the major groove is considerably larger for the ions with higher charge. For instance, the peak in the counterion concentration within the major and the minor grooves are about 4.5 and 3 M, respectively, for the monovalent cations; the corresponding values for the trivalent counterions are 3 and 1 M.

The helical projection for the coions distribution is shown in Fig. 5. The preferred positions for the coions are the center of the grooves. But they are mostly located outside of the minor groove, whereas they may be found both inside and outside the major groove. In fact, the highest population of coions is found in the middle of the major groove only

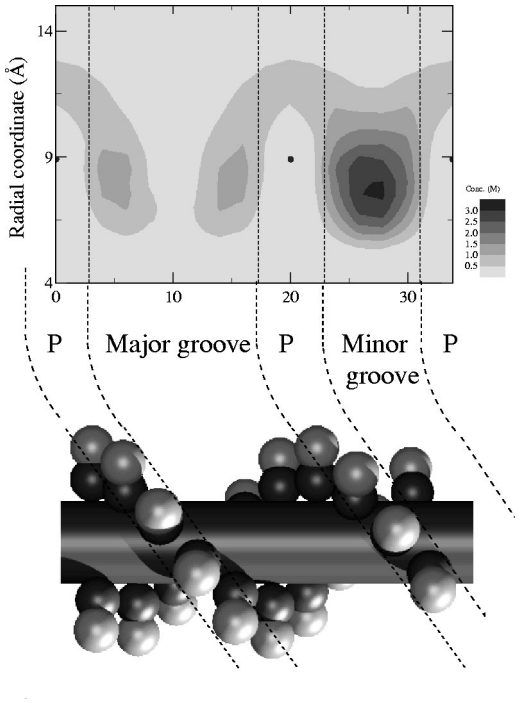

FIG. 4. Helical projection (see Ref. 2) of the counterion concentration for the system containing 3:1 added salt at 0.003 M concentration. The GP model has been depicted to sketch the meaning of the axial coordinate in the helical projection. The phosphates (represented by a dot in the higher plot), major groove, and minor groove regions are delimited by dashed lines.

slightly shifted from the phosphates radial coordinate (at 10 Å). There, the coion concentration is about *twice the bulk value*. The presence of anions so close to the negatively charged phosphate groups could be quite surprising, but it can be explained by the salt bridges phosphate–counterion–coion commented above in relation with the maximum in the coions concentration profile. We have observed that, in many cases, the bridge involves five ions, P–counterion–coion–counterion–P, connecting both sides of the major groove. Notice also that the salt bridges are not exclusive of DNA with added 3:1 salt; they have also been observed in simple electrolyte solutions containing divalent ions[34,35] and in all of our GP simulations irrespective of the charge of the mobile ions. What makes the case of trivalent cations around DNA peculiar is that the salt bridges affect the coions distribution so deeply that this function reaches a local maximum.

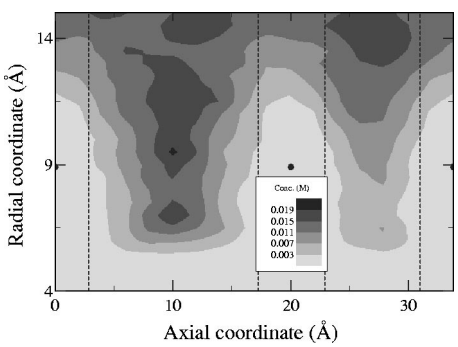

FIG. 5. Coions concentration (helical projection) for the system containing 3:1 added salt at 0.003 M concentration.

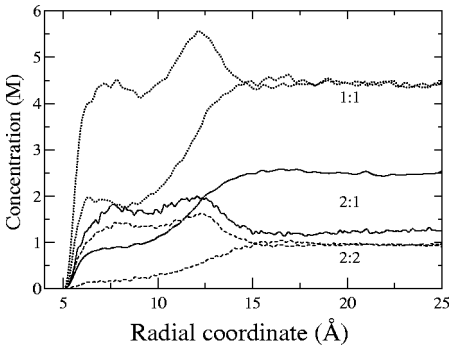

FIG. 6. Concentration profiles for systems containing 1:1 (dotted lines), 2:1 (full lines), and 2:2 (dashed) added salts at 4 M ionic strength.

B. Systems at high ionic strength

In this section we investigate the distribution of ions around DNA immersed in 1:1, 2:1 (cation:anion) and 2:2 electrolytes at a ionic strength about 4 M. The concentration profiles are presented in Fig. 6. In contrast with the behavior at low salt, the ionic distributions in the vicinity of the polyion are strongly dependent on their bulk values and the height of the peaks are no longer similar. A plot of the concentration profiles relative to the bulk concentration may help to extract the significant structural features. Such functions are displayed in Fig. 7. The relative penetration of the divalent cations is quite similar in the 2:1 and the 2:2 systems and, as expected, it is larger than that of the monovalent cations. Coherently, the relative penetration of coions decreases with the charge of the anion. Although the ionic concentration profiles of the asymmetrical electrolyte are essentially determined by the charge of its components, there are small but significant departures between the relative profiles of ions carrying the same charge but belonging to different salts. It can be seen in Fig. 7 that the bulk relative concentration of the divalent counterions for the asymmetric salt is lower than that for the symmetrical one whereas for the monovalent coions the opposite is true. In other words, the ionic distributions of the asymmetric salt are bracketed by the corresponding functions of the symmetric electrolytes.

At the scale of Figs. 6 and 7 it is difficult to realize that the coion concentration profiles of the three systems have a maximum at about 17 Å. Besides, the counterion and coion curves cross at about 15 Å. This means that beyond such a

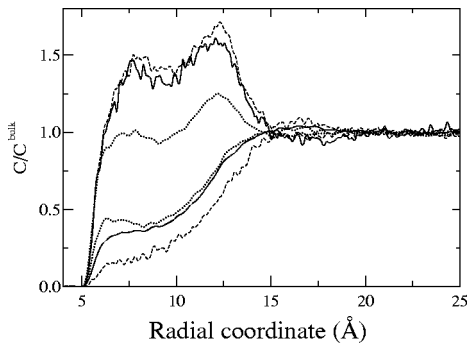

FIG. 7. The concentration profiles relative to the bulk values for the systems of Fig. 6.

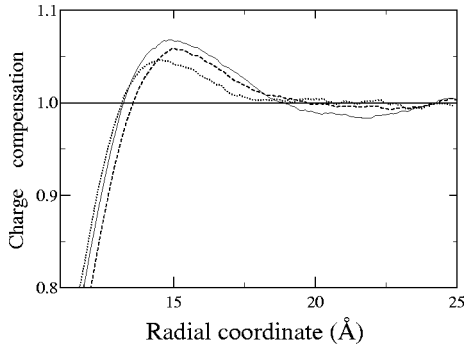

FIG. 8. Charge compensation functions for systems containing 1:1 (dotted lines), 2:1 (full lines), and 2:2 (dashed) added salts at 4 M ionic strength.

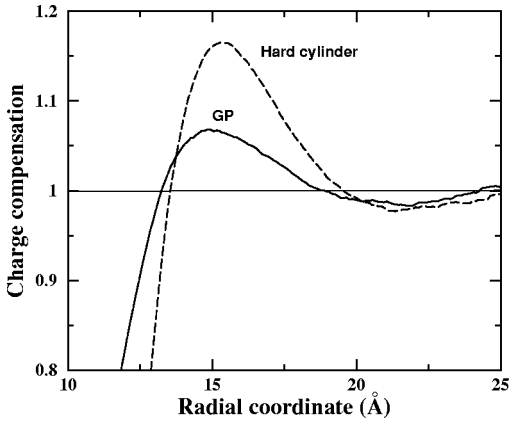

FIG. 9. Charge compensation functions for the GP model (full line) and a hard charged cylinder (dashed). In both cases, the systems contain 2:1 added salt at 4 M ionic strength.

distance to the axis the average local charge has the same sign as the polyion, i.e., there is a local inversion of the usual charge sign in the solution. This feature likely denotes the cancellation of a previous overscreening of the DNA charge by the counterions. The occurrence of a maximum in the charge compensation functions—see Fig. 8—confirms our assertion. The maximum appears in the three systems indicating that the charge reversal takes place *only* in systems at high ionic strength *irrespective* of the electrovalence of the mobile ions (cf. Fig. 2). The charge of the cation plays only a secondary role in this effect; in particular, the height of the maximum is slightly higher for the solutions containing divalent counterions. Besides, a clear minimum at 22 Å can be observed in the solutions with divalent counterions whereas we cannot assert its appearance with monovalent salt.

It may seem surprising that both the maximum and the minimum of the charge compensation functions are more marked in the 2:1 solution than in the 2:2 system. This behavior is the opposite to what would be expected by considering exclusively the (negative) electrostatic potential created by the polyion since this one would hamper the (negatively charged) monovalent coions to a lesser degree than the divalent ones. But, as the counterions condense around the polyion, its charge is eventually overneutralized so the coions should undergo a net *attractive* potential and the divalent anions may approach this region more easily than the ions carrying unity negative charges. The final conclusion is that the charge inversion should be somewhat damped as the charge of the anion is increased. This conclusion is consistent with the fact that the peak in the coion concentration profiles (see the region beyond 15 Å in Fig. 7) is higher for the 2:2 salt system than for the asymmetric one.

The conclusion of the previous paragraph is that the overscreening of the polyion charge favors the approach of highly charged coions. The arguments may be easily extended to systems in which the coions charge is very large. In the limit when the coion charge (and size) becomes identical to that of the macroion at the origin, the ''coions'' would be strongly attracted by the ionic envelope of the latter and both macroions would approach merging their counterion clouds. The result would be a net *attraction* between the like-charged macroions at certain distances.

It is interesting to compare the results for the grooved DNA model to those obtained with a more simple model such a homogeneously charged hard cylinder. The charge compensation functions for both models are depicted in Fig. 9. In accordance with what happened in the case of added monovalent salt,[1] the hard body leads to a noticeable enhancement of the charge reversal for the 2:1 system. This effect has also been observed in studies of DNA fibers using a uniformly charged cylinder and a mixed cylindrical–helical model that allows the penetration of ions into the grooves.[36] A plausible reason for this behavior is that the penetration of counterions within the grooves screen the polyion, thus reducing its effective charge. The strong screening of the phosphates charge has also been argued to explain the weak effect of the image interactions in DNA.[25] Notice finally the apparent contradiction that the ''less structure'' observed in the GP model (in the sense that its charge compensation function has a less developed maximum and minimum) comes, in fact, from a more complex organization of the ions, which is dependent on the shape of the molecule and on the position of the DNA charges.

C. Mixtures of salts with divalent and monovalent cations

In previous sections we have analyzed the distinct behavior of ions carrying different charges. But the comparisons have been done for separated systems, i.e., the ions were not together in the same solution. In this section we investigate the direct competition of cations with different valences when they are put together within the same solution. In particular, the solution contains three sorts of ions with charges $+2,+1,-1$ (2:1:1 electrolyte). The selected ionic strength—about 0.12 M—was chosen for its pertinence to biological conditions. We deal with two mixtures that differ only in the ratio between the bulk concentrations of the monovalent cation to the divalent one, about 32 and 9, respectively. The concentration profiles are displayed in Figs. 10 and 11. In the former system, the height of the maximum is quite similar for the monovalent and the divalent cations (0.75 and 0.70 M, respectively) despite the great difference in their bulk concentrations. Besides, the concentration profile of the monovalent counterions is lower than that of a 1:1 system at the same ionic strength (see Fig. 10). The con-

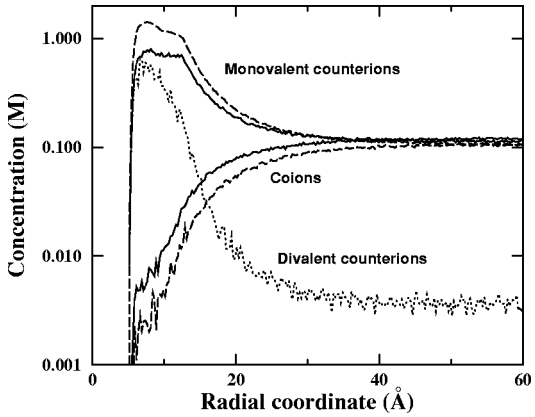

FIG. 10. Concentration profiles for a 2:1:1 system containing a mixture of divalent and monovalent counterions and a monovalent coion. The dotted line is for the divalent cations and the full line is for both types of monovalent ions. The ratio of the monovalent/divalent counterion bulk concentrations is about 32. Results for a 1:1 added salt at the same ionic strength are also included (dashed lines) for comparison. The scale is logarithmic.

densed divalent counterions ''squeeze'' the monovalent cations out of the charged polyion even if they are a minority component of the system. This fact was qualitatively described in earlier PB calculations for a homogeneously charged cylinder,[16] but the magnitude of the effect was severely underestimated. It has been explained as due to the lower entropic cost required to associate *one* divalent ion with respect to *two* monovalent cations.[20] Later on, this feature has been confirmed by computer simulation studies, both at infinite salt dilution,[18] and in systems with added salt as well.[37,38]

When the ratio monovalent/divalent counterion concentration decreases, the peak of the concentration profile for the divalent cations increases. In the system with a ratio of about 9, the height of the divalent counterions peak is more than *twice* that of the monovalent ones in spite of the fact that its bulk concentration is one order of magnitude lower. Another effect of the presence of highly charged cations is to compact the region of ionic inhomogeneity around the polyion: the concentration of the monovalent counterions is essentially the same as that of the coions at 30 Å in the 2:1:1 system while the same occurs beyond 40 Å for 1:1 added salt at the same ionic strength. This also occurs in the system with a monovalent/divalent ratio of 32 and it may also be observed in the above cited simulation references but does not agree with the CC theory, which predicts a larger Manning radius for divalent cations.

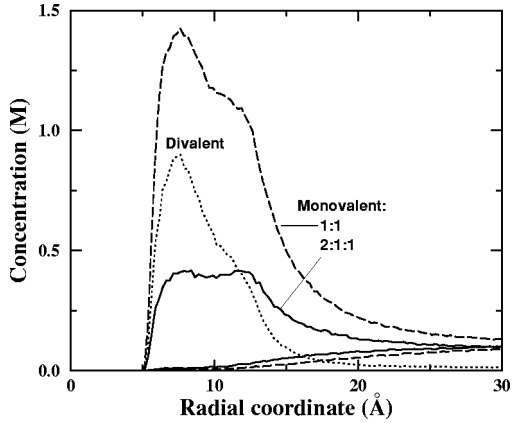

FIG. 11. The same as Fig. 10 but for the system with a 9.3 monovalent/divalent counterion bulk concentrations ratio. The scale is linear.

IV. DISCUSSION

As commented on in the Introduction, the conclusions of this work may be relevant at two different levels. The first concerns the influence of the presence of multivalent ions on DNA properties and the ability of the GP model to predict them. In our previous papers I and II we have shown the importance of the polyelectrolyte shape on the distribution of monovalent counterions around DNA. In this work we have seen that the presence of multivalent counterions enhances the formation of salt bridges. Besides, the multivalent cations squeeze the monovalent ones out of the charged polyion vicinity. One of the most important effects of the addition of salt to DNA is the possibility to provoke conformational changes, from B- to Z- or A-DNA. We have demonstrated[5] that the penetration of ions into the grooves is mostly responsible for the strong dependence of the B-→Z-DNA free energy difference on the concentration of monovalent added salts. Thus, the displacement of the monovalent counterions by the multivalent ones should result in a deeper dependence of the free energy difference with salt concentration. As a consequence, the midpoint concentration (that at which both conformers are equally probable) decreases in the GP model from about 3.5 M (monovalent counterions) to 0.65 M (divalent).[39,40] This is in accordance with the experimental findings. In fact, the agreement of the simulation results for the midpoint concentration of the GP model is not only qualitative but also quantitative. This was not expected because the model relies on two important simplifications at the electrostatic level. It was already pointed out by Skolnick and Fixman[41] that the dielectric discontinuity effect may not be as important as one would naively expect. The results of the present paper seem to confirm the suggestion of MPB calculations[25] that the strong screening of the phosphates charge may explain the weak effect of the image interactions in DNA. On the other hand, other MPB results[42] indicate that the effect of the dielectric saturation cannot be completely neglected. Similar conclusions were obtained in the analysis of the simulation results for the B-→Z-DNA transition.[5] This seems a major lack of our model that, unfortunately, has a difficult solution because of the huge amount of computation required to deal with more refined models both at the theoretical and the simulation level.

On the other hand, in this paper we may provide some insights into the understanding of highly charged macroions in solution in general and, in particular, into the problem of counterion mediated attraction between like-charged macroions.[10,12–14,43,44] The occurrence of either a charge inversion or a maximum in the coions profile in our system is clearly a hint of a possible attraction between like-charged macroions in analogous conditions. The crucial point is how our results for a system made of a polyion at infinite dilution with added salt may be extrapolated to systems for which the concentration of macroion is non-negligible. A first approxi-

mation linking both systems is the so-called cell model in which the system is partitioned into cells, each containing one macroion together with its neutralizing counterions. In the cell model, the counterion concentration at the cell limit plays an analogous role as the bulk concentration determined by the added salt in the infinitely diluted polyion. On the other hand, an increase of the macroion concentration implies a corresponding increase in the number of released counterions and, thus, it produces a similar effect as the addition of salt in our system. But, as long as one is interested in the interaction between macroions, the cell model should not be invoked beyond that similarity. In fact, from the point of view of each polyion, the remainder macroions are simply highly charged coions. We have shown in this work that, for a given counterion charge, the occurrence of a maximum in the coions profile is enhanced by increasing the charge of the coions. In other words, even in the case of monovalent counterions, DNA chains should attract each other when the concentration of the released counterions is lower than that leading to charge reversal in the corresponding cell model, which, in turn, must be approximately the same as that producing overscreening in an infinitely diluted polyion with added salt. The results of this and previous works indicate that the concentration of the released counterions at the cell limit should be of the order of 1 M for the attraction between macroions to take place. Interestingly, the mean concentration of counterions in the condensed state of DNA (fibers) is 1–2 M for distances between the DNA helix axes of about 20–40 Å.[36] The extrapolation of our results for the 3:1 salt (where a maximum in the coions profile appears at added salt ionic strengths as low as 0.02 M) indicate that DNA should condense almost irrespective of its concentration when in the presence of trivalent counterions. These conclusions are in accordance with experimental findings in DNA solutions.

ACKNOWLEDGMENT

This work was supported in part by the DGES-SEUI (Spain), Grant No. PB97-0258-C02-01.

[1] J. C. Gil Montoro and J. L. F. Abascal, J. Chem. Phys. **103**, 8273 (1995).
[2] J. C. Gil Montoro and J. L. F. Abascal, J. Chem. Phys. **109**, 6200 (1998).
[3] J. C. Gil Montoro, Ph.D. thesis, Universidad Complutense de Madrid, 1997.
[4] J. C. Gil Montoro and J. L. F. Abascal, J. Chem. Phys. **106**, 8239 (1997).
[5] J. L. F. Abascal and J. C. Gil Montoro, J. Chem. Phys. **110**, 11094 (1999).
[6] M. A. Young, B. Jayaram, and D. L. Beveridge, J. Am. Chem. Soc. **119**, 59 (1997).
[7] A. P. Lyubartsev and A. Laaksonen, J. Biomol. Struct. Dyn. **16**, 579 (1998).
[8] V. A. Bloomfield, Biopolymers **31**, 1471 (1991).
[9] R. Podgornik, D. Rau, and V. Parsegian, Biophys. J. **66**, 962 (1994).
[10] L. Guldbrand, L. G. Nilsson, and L. Nordenskiöld, J. Chem. Phys. **85**, 6686 (1986).
[11] A. P. Lyubartsev and L. Nordenskiöld, J. Phys. Chem. **99**, 10373 (1995).
[12] J. X. Tang, S. Wong, P. T. Tran, and P. A. Janmey, Ber. Bunsenges. Phys. Chem. **100**, 796 (1996).
[13] N. Grønbech-Jensen, R. J. Mashl, R. F. Bruinsma, and W. M. Gelbart, Phys. Rev. Lett. **82**, 101 (1999).
[14] M. J. Stevens, Phys. Rev. Lett. **82**, 101 (1999).
[15] P. Sottas, E. Larquet, A. Stasiak, and J. Dubochet, Biophys. J. **77**, 1858 (1999).
[16] D. Dolar and A. Peterlin, J. Chem. Phys. **50**, 3011 (1969).
[17] G. S. Manning, Q. Rev. Biophys. **11**, 179 (1978).
[18] M. Le Bret and B. H. Zimm, Biopolymers **23**, 271 (1984).
[19] P. N. Vorontsov-Velyaminov and A. P. Lyubartsev, J. Biomol. Struct. Dyn. **7**, 739 (1989).
[20] R. J. Bacquet and P. J. Rossky, J. Phys. Chem. **92**, 3604 (1988).
[21] C. W. Outhwaite, J. Chem. Soc., Faraday Trans. 2 **82**, 789 (1986).
[22] T. Das, D. Bratko, L. B. Bhuiyan, and C. W. Outhwaite, J. Phys. Chem. **99**, 410 (1995).
[23] T. Das, D. Bratko, L. B. Bhuiyan, and C. W. Outhwaite, J. Chem. Phys. **107**, 9197 (1997).
[24] S. Gavryushov and P. Zielenkiewicz, J. Phys. Chem. B **101**, 10903 (1997).
[25] S. Gavryushov and P. Zielenkiewicz, Biophys. J. **75**, 2732 (1998).
[26] W. Saenger, *Principles of Nucleic Acid Structure* (Springer-Verlag, New York, 1984).
[27] S. Arnott and D. W. L. Hukins, Biochem. Biophys. Res. Commun. **47**, 1504 (1972).
[28] J. C. Gil Montoro and J. L. F. Abascal, Mol. Phys. **89**, 1081 (1996).
[29] R. M. Fuoss, A. Katchalsky, and S. Lifson, Proc. Natl. Acad. Sci. U.S.A. **37**, 579 (1951).
[30] J. C. Gil Montoro and J. L. F. Abascal, Mol. Simul. **14**, 313 (1995).
[31] J. C. Gil Montoro and J. L. F. Abascal, Mol. Simul. **21**, 249 (1999).
[32] C. L. Brooks, B. M. Pettitt, and M. Karplus, J. Chem. Phys. **83**, 5897 (1985).
[33] H. L. Gordon and S. Goldman, Mol. Simul. **3**, 213 (1989).
[34] J. L. F. Abascal and P. Turq, Chem. Phys. **153**, 79 (1991).
[35] J. L. F. Abascal, F. Bresme, and P. Turq, Mol. Phys. **81**, 143 (1994).
[36] N. Korolev, A. P. Lyubartsev, A. Rupprecht, and L. Nordenskiöld, J. Phys. Chem. B **103**, 9008 (1999).
[37] C. S. Murthy, R. J. Bacquet, and P. J. Rossky, J. Phys. Chem. **89**, 701 (1985).
[38] P. N. Vorontsov-Velyaminov and A. P. Lyubartsev, Mol. Simul. **9**, 285 (1992).
[39] J. L. F. Abascal and J. C. Gil Montoro, J. Phys.: Condens. Matter **12**, A327 (2000).
[40] J. L. F. Abascal and J. C. Gil Montoro, to be published.
[41] J. Skolnick and M. Fixman, Macromolecules **11**, 867 (1978).
[42] S. Gavryushov and P. Zielenkiewicz, J. Phys. Chem. B **103**, 5860 (1999).
[43] M. Olvera de la Cruz *et al.*, J. Chem. Phys. **103**, 5781 (1995).
[44] B.-Y. Ha and A. J. Liu, Phys. Rev. Lett. **79**, 1289 (1997).